Particle dynamics

Plasma Physics and
Controlled Fusion

TUTORIAL • **OPEN ACCESS**

Particle dynamics

To cite this article: I Pusztai and R J Hastie 2026 *Plasma Phys. Control. Fusion* **68** 053301

Plasma Physics and Controlled Fusion

TUTORIAL

Particle dynamics

OPEN ACCESS

RECEIVED
21 February 2026

REVISED
12 April 2026

ACCEPTED FOR PUBLICATION
27 April 2026

PUBLISHED
11 May 2026

I Pusztai[1,*] and R J Hastie[2]

[1] Department of Physics and Astronomy, Chalmers University of Technology, Gothenburg SE-41296, Sweden
[2] Culham Centre for Fusion Energy, Culham Science Centre, Abingdon OX 14 3DB Oxon, United Kingdom
[*] Author to whom any correspondence should be addressed.

E-mail: pusztai@chalmers.se

Keywords: particle dynamics, basic plasma physics, tutorial, adiabatic invariants

Abstract

This article provides an introduction to kinetic plasma physics through the theory of charged particle motion in prescribed, inhomogeneous, and time-dependent electromagnetic fields. Starting from the exact solution in uniform, static fields, we identify the fundamental spatial and temporal scales of magnetized motion—the Larmor radius and cyclotron frequency—which enable systematic expansions when the electromagnetic fields vary slowly compared with these intrinsic scales. Under this drift (adiabatic) ordering, particle dynamics separates into rapid gyromotion and slower guiding-centre motion. We derive the guiding-centre equations by progressively incorporating spatial and temporal field variations and examine the emergence of adiabatic invariants, including conservation of the magnetic moment and higher-order corrections obtained perturbatively. Applications to tokamak geometry illustrate the implications for magnetic confinement. Finally, we briefly discuss extensions beyond the ideal collisionless picture, including Debye shielding, radiation reaction, and the effects of collisions and turbulence.

1. Introduction

In this chapter we develop the theory for the orbits of the constituent charged particles of a high temperature plasma in inhomogeneous and time dependent electromagnetic fields, assumed known. Starting from uniform and static fields, it is shown how these fields define a characteristic length, r_L, and a characteristic frequency, ω_c, and that solutions in more general fields can be developed as expansions in two small parameters, r_L/L and ω/ω_c, where L and ω are the characteristic length scale and frequency scale for the variation of these electromagnetic fields.

In high temperature plasmas, where collisional encounters between the constituent charged particles are rare, an understanding of plasma phenomena requires a knowledge of the individual particle trajectories in the presence of electric and magnetic fields. Although the particles represent charges and currents and a self-consistent evaluation of the fields is sometimes challenging, in this chapter we will assume them to be given functions of space and time.

Only in highly symmetric fields can exact solutions of the equations of motion of a charged particle be obtained. For instance, in a constant uniform magnetic field a charged particle trajectory is a simple helix with its axis parallel to the magnetic field $\boldsymbol{B}$. However, this simple orbit defines a fundamental frequency, the cyclotron frequency (also called Larmor frequency or gyro-frequency), $\omega_c = ZeB/m$, and a fundamental length, the Larmor radius, $r_L = v_\perp/\omega_c$. Here, m and Ze are the mass and charge of the particle, with e the elementary charge, and $v_\perp$ is the particle speed perpendicular to the field line, to be defined more rigorously later.

When considering trajectories in inhomogeneous and time dependent electromagnetic fields it is frequently the case that the characteristic time and length scales over which these fields vary are much greater than $1/\omega_c$ and r_L. In this chapter we will show how, when this is true, the trajectories of individual charged particles can be obtained by expansions in ω/ω_c and r_L/L, where ω and L are characteristic of the temporal and spatial variations in the fields. Such an approximation is often referred to as the drift, or adiabatic approximation. The charged particle motion can then be split into a local helical

gyration around a field line, and the motion of the *guiding centre*, that is the instantaneous centre of this gyration.

We will first present a heuristic derivation of the equations governing the guiding centre motion in section 2. Starting from the simplest case of homogeneous and time-independent fields in section 2.1, we will successively increase the complexity by introducing temporal and various types of spatial variations of the fields. In this way, we will find various components of the guiding centre motion in sections 2.2–2.6.

In section 3 we will consider the problem of adiabatic invariants—approximate constants of motion, which arise when particles exhibit periodic motion. First we will show that the magnetic moment of a charged particle remains unchanged in the presence of slowly time-varying and spatially varying fields, in sections 3.1 and 3.2, respectively. Then we will employ a perturbative method that allows us to find further adiabatic invariants and higher order corrections to adiabatic invariants, in section 3.3. To better illustrate concepts related to guiding centre motion and adiabatic invariants, we devote section 3.4 to a consideration of particle trajectories in tokamak fusion devices.

After a brief discussion of radiation reaction effects on particle dynamics in section 4, we will go beyond the simple particle picture, and consider collective phenomena. A basic property of plasma, that it is very nearly charge neutral macroscopically, will be found as the consequence of the Debye screening phenomena, discussed in section 5. Finally, we will provide some insights to how particle orbits are affected by collisions and turbulent fluctuations in section 6.

2. Particle motion in magnetized plasmas

In this section we consider the motion of a single, non-relativistic, charged particle in given electric and magnetic fields. We shall see that, in the presence of a strong magnetic field, the particle motion consists of a fast Larmor gyration (cyclotron motion) superimposed on a slower drift motion across the magnetic field, plus the parallel motion. This observation motivates us to introduce the concept of the guiding centre, that is a fictitious point around which the particle gyrates. Here we will mainly focus on the particle dynamics perpendicular to the field lines, and the discussion of the parallel dynamics will be completed in section 3 once the effects of the magnetic mirror force are introduced.

Our analysis starts with the equations of motion for a charged particle in the presence of the electric and magnetic fields, $\boldsymbol{E}$ and $\boldsymbol{B}$

$$\dot{\boldsymbol{v}} = \frac{Ze}{m}[\boldsymbol{E} + (\boldsymbol{v}\times\boldsymbol{B})], \tag{2.1}$$

$$\dot{\boldsymbol{x}} = \boldsymbol{v}. \tag{2.2}$$

Since we will frequently resolve vectors into components parallel to, and perpendicular to $\boldsymbol{B}$, we introduce the following notation

$$\hat{\boldsymbol{b}} = \frac{\boldsymbol{B}}{B}, \qquad v_\parallel = \boldsymbol{v}\cdot\hat{\boldsymbol{b}}, \qquad \boldsymbol{v}_\perp = \boldsymbol{v} - v_\parallel\hat{\boldsymbol{b}}, \qquad v_\perp = |\boldsymbol{v}_\perp|, \tag{2.3}$$

and similarly for other vectors, such as $\boldsymbol{E}$, $\boldsymbol{\nabla}$, etc.

2.1. Constant, uniform fields

We first assume uniform and time-independent electric and magnetic fields with arbitrary relative orientation. Taking the parallel component of equation (2.1), we find

$$\dot{v}_\parallel = \frac{Ze}{m}E_\parallel \qquad \Rightarrow \qquad v_\parallel = \frac{Ze}{m}E_\parallel t + \text{const.}, \tag{2.4}$$

describing free acceleration along the magnetic field direction if $E_\parallel \neq 0$. The perpendicular component of equation (2.1)

$$\frac{m}{Ze}\dot{\boldsymbol{v}}_\perp = \boldsymbol{E}_\perp + \boldsymbol{v}_\perp\times\boldsymbol{B} \tag{2.5}$$

describes the application of a force $\boldsymbol{F} = Ze\boldsymbol{E}_\perp$ to a particle, but unlike the application of the longitudinal force $ZeE_\parallel$ this does not result in free acceleration of the particle, as can be seen by transforming from $\boldsymbol{v}_\perp$ to the new velocity variable $\boldsymbol{c}_\perp$,

$$\boldsymbol{v}_\perp = \boldsymbol{c}_\perp + \boldsymbol{V}_E, \tag{2.6}$$

where $\boldsymbol{V_E} = (\boldsymbol{E}\times\boldsymbol{B})/B^2$ is a constant velocity. Equation (2.5) then takes the form

$$\frac{m}{Ze}\dot{\boldsymbol{c}}_\perp = \boldsymbol{c}_\perp \times \boldsymbol{B}. \tag{2.7}$$

Now taking the scalar product of equation (2.7) with $\boldsymbol{c}_\perp$, we have

$$\boldsymbol{c}_\perp\cdot\dot{\boldsymbol{c}}_\perp = \frac{1}{2}\frac{\mathrm{d}\left(c_\perp^2\right)}{\mathrm{d}t} = 0, \tag{2.8}$$

that is there is no increase in the perpendicular energy of the particle. Using equation (2.7) a second time, and making use of the vector identity $\boldsymbol{A}\times(\boldsymbol{B}\times\boldsymbol{C}) = \boldsymbol{B}(\boldsymbol{A}\cdot\boldsymbol{C}) - \boldsymbol{C}(\boldsymbol{A}\cdot\boldsymbol{B})$, one finds

$$\ddot{\boldsymbol{c}}_\perp = -\left(\frac{ZeB}{m}\right)^2 \boldsymbol{c}_\perp, \qquad \text{or,} \qquad \ddot{\boldsymbol{c}}_\perp = -\omega_\mathrm{c}^2\boldsymbol{c}_\perp. \tag{2.9}$$

Consequently each component of $\boldsymbol{c}_\perp$ satisfies the equation of the simple harmonic oscillator with frequency $\omega_\mathrm{c} = ZeB/m$. This is known as the cyclotron frequency, gyro-frequency, or Larmor frequency.

Introducing a Cartesian coordinate system $\{x, y, z\}$ with the z-axis in the direction of $\hat{\boldsymbol{b}}$, we have

$$\begin{aligned} c_x &= c_\perp\cos\left(\omega_\mathrm{c}t+\varphi\right), \\ c_y &= -c_\perp\sin\left(\omega_\mathrm{c}t+\varphi\right), \end{aligned} \tag{2.10}$$

with the phase φ an arbitrary constant. Returning to equation (2.2), it follows that $\boldsymbol{x}_\perp$ undergoes a cross-field drift (in response to $\boldsymbol{E}_\perp$) together with circular motion around this drifting 'guiding centre'.

$$\begin{aligned} x &= \frac{c_\perp}{\omega_c}\sin\left(\omega_c t+\varphi\right) + x_c\left(t\right), \\ y &= \frac{c_\perp}{\omega_c}\cos\left(\omega_c t+\varphi\right) + y_c\left(t\right), \end{aligned} \tag{2.11}$$

where the cross-field drift motion of the guiding centre is given by

$$\begin{aligned} \frac{\mathrm{d}x_c}{\mathrm{d}t} &= V_{Ex} = \frac{E_y}{B}, \\ \frac{\mathrm{d}y_c}{\mathrm{d}t} &= V_{Ey} = -\frac{E_x}{B}. \end{aligned} \tag{2.12}$$

The position $\boldsymbol{x}_\mathrm{c}(t)$ of the centre about which the particle gyrates is known as the guiding centre, and its velocity (in this very simple case the constant velocity V_E) is referred to as the drift velocity of the guiding centre. The frequency of gyration is again ω_c, and the radius of gyration, the Larmor radius, is

$$r_\mathrm{L} = \left|\left(\boldsymbol{x}-\boldsymbol{x}_\mathrm{c}\right)_\perp\right| = \frac{c_\perp}{\omega_\mathrm{c}}. \tag{2.13}$$

Thus, whereas a constant longitudinal electric field, $E_\parallel$, results in free acceleration of a charged particle, application of a constant electric field perpendicular to $\boldsymbol{B}$ results in a steady cross field drift, $\boldsymbol{V_E}$, of the particle. This drift can be qualitatively understood by considering the change in perpendicular velocity $v_\perp$ in the direction of $E_\perp$ within one gyro-period, and the corresponding variation in the local value of the Larmor radius (i.e. equation (2.13) with $c_\perp \to v_\perp$). We note that in the inertial frame moving with the velocity $\boldsymbol{V_E}$, the electric field is zero (see figure 1), and the magnetic field remains almost unchanged if the particle motion is non-relativistic, as can be shown by Lorentz transforming the fields. In uniform fields the effect of the electric field can be completely transformed away this way, while in the presence of curved magnetic fields the frame where $\boldsymbol{E}$ vanishes is a rotating frame; in this case additional inertial forces arise that affect the particle dynamics.

Finally, we note that, if some additional force $\boldsymbol{F}$ acts on the particle, the foregoing analysis holds with $\boldsymbol{E}$ replaced by $\boldsymbol{F}/(Ze)$. Thus the effect of such a transverse force will be to produce an additional guiding centre drift velocity

$$\frac{1}{Ze}\frac{\boldsymbol{F}\times\boldsymbol{B}}{B^2}. \tag{2.14}$$

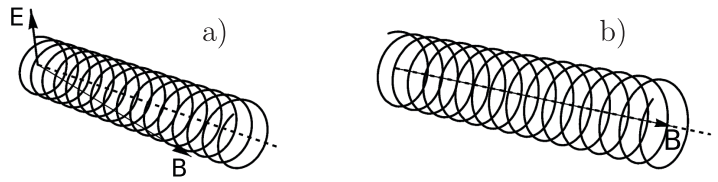

Figure 1. Charged particle motion in uniform $\boldsymbol{B}$ and $\boldsymbol{E}$ fields, assuming $\boldsymbol{E}\perp\boldsymbol{B}$. (a) Laboratory frame ($\boldsymbol{E}\neq 0$). (b) in frame moving with velocity $\boldsymbol{V}_{\boldsymbol{E}}$ ($\boldsymbol{E}=0$ in this frame). Dashed lines represent the guiding centre trajectory.

2.2. Slow temporal and spatial variations

The importance of understanding in detail the motion of a charged particle in constant uniform fields lies in the fact that, for many cases of interest, both in the plasmas of fusion devices and in naturally occurring plasmas, the scale of the inhomogeneity of the fields, L, is very large compared to a Larmor radius, r_{L}, and the time scale of interest, T, is very long when compared to a gyro-period, $2\pi/\omega_{\mathrm{c}}$. Under these conditions particle trajectories can be separated into a rapid gyration around the position of the guiding centre and the motion of the guiding centre itself, both along and across the field, where its transverse velocity takes the form of a slow drift motion. If, in addition, the frequency of collisions between plasma particles is much smaller than ω_{c}, the plasma is *magnetized*. In the rest of this section we present a simple derivation of these effects, assuming $r_{\mathrm{L}}/L\ll 1$ and $2\pi/(\omega_{\mathrm{c}}T)\ll 1$. To complete our discussion of the guiding centre motion, in section 3 we will describe a method for obtaining the particle orbits as a systematic expansion in the small parameters $r_{\mathrm{L}}/L\ll 1$ and $2\pi/(\omega_{\mathrm{c}}T)\ll 1$. Such expansion procedures form a basis for the gyrokinetic theory (see Abel *et al* (2013) and references therein), which is widely used to describe transport processes in magnetized laboratory or space plasmas.

2.3. Time-varying electric field

We assume here that $\boldsymbol{E}$ is perpendicular to $\boldsymbol{B}$ and spatially uniform. Transforming as before, to a frame moving with velocity $\boldsymbol{V}_{\boldsymbol{E}}=\boldsymbol{E}\times\boldsymbol{B}/B^2$, we have $\boldsymbol{v}_\perp=\boldsymbol{V}_{\boldsymbol{E}}+\boldsymbol{c}_\perp$, and

$$\frac{m}{Ze}\dot{\boldsymbol{c}}_\perp=-\frac{m}{Ze}\dot{\boldsymbol{V}}_{\boldsymbol{E}}+\boldsymbol{c}_\perp\times\boldsymbol{B}. \tag{2.15}$$

This equation has a structure similar to that of equation (2.5), but with the property that the additional force term is of order $(1/\omega_{\mathrm{c}})(\mathrm{d}E/\mathrm{d}t)$ and is therefore of order $\mathcal{O}(\omega/\omega_c)E$, where ω characterizes the time variation of $E(t)$. Now introducing a second transformation to a frame moving with velocity

$$\boldsymbol{V}_{\dot{\boldsymbol{E}}}=\frac{1}{\omega_{\mathrm{c}}}\frac{\dot{\boldsymbol{E}}}{B}, \tag{2.16}$$

thus $\boldsymbol{c}_\perp=\boldsymbol{f}_\perp+\boldsymbol{V}_{\dot{\boldsymbol{E}}}$, equation (2.15) becomes

$$\frac{m}{Ze}\dot{\boldsymbol{f}}_\perp=\boldsymbol{f}_\perp\times\boldsymbol{B}-\frac{\ddot{\boldsymbol{E}}}{\omega_{\mathrm{c}}^2}. \tag{2.17}$$

Here, the term involving $\ddot{\boldsymbol{E}}$ is now of order $(\omega/\omega_{\mathrm{c}})^2$ and can be neglected since it is of second order in the small expansion parameter. The equation for $\boldsymbol{f}$ then assumes the familiar form describing Larmor gyration. Thus averaging the total motion over a gyro-period we obtain the guiding centre velocity,

$$\begin{aligned}\langle\boldsymbol{v}\rangle&=v_\parallel\hat{\boldsymbol{b}}+\frac{\boldsymbol{E}\times\boldsymbol{B}}{B^2}+\frac{1}{\omega_{\mathrm{c}}}\frac{\dot{\boldsymbol{E}}}{B}\\&=v_\parallel\hat{\boldsymbol{b}}+\boldsymbol{V}_{\boldsymbol{E}}+\boldsymbol{V}_{\dot{\boldsymbol{E}}},\end{aligned} \tag{2.18}$$

where $\langle X\rangle\equiv\oint X\mathrm{d}\varphi$ denotes the gyro-average, and $\langle\boldsymbol{f}_\perp\rangle=0$ to the order of interest in $\omega/\omega_{\mathrm{c}}$, by construction. The new drift velocity, $\boldsymbol{V}_{\dot{\boldsymbol{E}}}$, known as the polarization drift, is charge-dependent, thus it causes charge separation. The polarization drift is illustrated in figure 2. The origin of this drift can also be understood by realizing that the frame moving with $\boldsymbol{V}_{\boldsymbol{E}}$ is not an inertial frame when $\dot{\boldsymbol{E}}\neq 0$. The inertial force $\boldsymbol{F}$ experienced by the particle in this accelerating frame causes a drift as given by equation (2.14), which recovers equation (2.16).

Evidently the procedure adopted in the foregoing analysis could be continued indefinitely, resulting in a series of drift velocities of order $(\omega/\omega_{\mathrm{c}})^n$. This example shows that the results obtained in varying $\boldsymbol{E}$

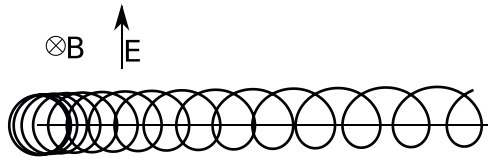

Figure 2. As $\dot{\boldsymbol{E}} \neq 0$ the particle undergoes a polarization drift (assuming $\dot{\boldsymbol{E}} \| \boldsymbol{E} \perp \boldsymbol{B}$). The guiding centre velocity can be decomposed as $\boldsymbol{v}_c = \boldsymbol{V}_E(t) + \boldsymbol{V}_{\dot{E}}$, where $\boldsymbol{V}_E$ is horizontal (along the straight solid line) and $\boldsymbol{V}_{\dot{E}}$ is vertical. Note that the gyroradius does not change in the process.

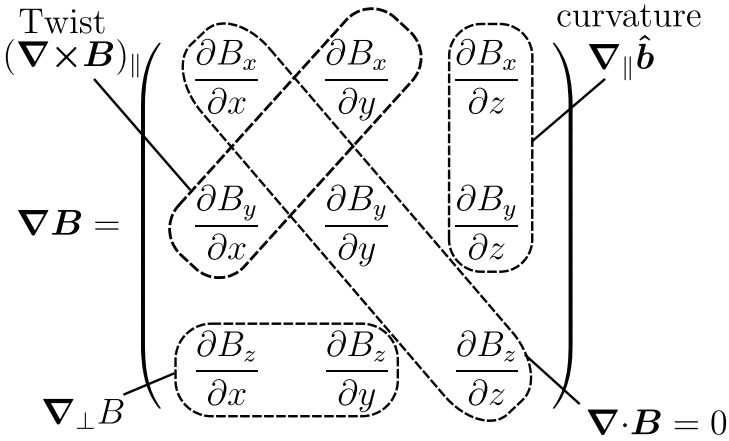

Figure 3. The $\nabla\boldsymbol{B}$ tensor in a Cartesian system with the z direction aligned with $\boldsymbol{B}$.

and $\boldsymbol{B}$ fields will only be approximate, and it gives a glimpse of a systematic method which can generate improved approximations. However, higher order corrections to the particle motion are not usually as easily obtained as in this simple case.

2.4. Magnetic field inhomogeneities

In the rest of section 2 we will assume that $\boldsymbol{E} = 0$ (implying a time independent $\boldsymbol{B}$ field) and consider the effects of magnetic field inhomogeneities on the guiding centre motion. We take a coordinate system $\{x, y, z\}$ with the z-direction along $\boldsymbol{B}$ at the particle guiding centre. This last statement is approximate, since gradients in B imply that the Larmor radius, r_L, must vary slightly in the course of each gyration, and therefore that the guiding centre itself must experience a small 'wobble'. Rigorous mathematical methods are available (Dubin *et al* 1983, Parra and Catto 2008) to construct a guiding centre position which has no gyro-frequency wobble to all orders in the small parameters, but we shall not pursue these methods here.

Because of the small Larmor orbit assumption ($r_L \ll L$), the fields experienced by the particle are dominated by B_z. Thus $|\boldsymbol{B}| \equiv B \simeq B_z$, and $\hat{\boldsymbol{b}}\cdot\nabla \simeq \partial/\partial z$. Consequently the terms $\partial_x B_z$ and $\partial_y B_z$ represent transverse gradients of B, $(\nabla_\perp B)$, while the term $\partial_z B_z$ represents the longitudinal gradient of B, $\nabla_\| B (\equiv \nabla_\| B - \nabla\cdot\boldsymbol{B} = -\partial_x B_x - \partial_y B_y)$, as illustrated in figure 3. The terms $\partial_z B_x$ and $\partial_z B_y$ represent change of direction of $\boldsymbol{B}$, i.e. field line curvature. The two remaining terms are related to $\hat{\boldsymbol{b}}\cdot(\nabla\times\boldsymbol{B}) = \mu_0 J_\|$ and to the torsion of magnetic field lines, but have a weaker effect on particle trajectories (μ_0 denotes the vacuum permeability).

2.5. Field line curvature

As a guiding centre moves along a curved field line, it experiences a centrifugal force

$$\boldsymbol{F} = -mv_\|^2\boldsymbol{\kappa} \equiv -\frac{mv_\|^2}{R_c}\boldsymbol{n}, \tag{2.19}$$

where $\boldsymbol{\kappa} = (\hat{\boldsymbol{b}}\cdot\nabla)\hat{\boldsymbol{b}}$ is curvature of the field line, R_c its radius of curvature, and $\boldsymbol{n}$ is the (inward pointing) unit vector. This force is perpendicular to $\boldsymbol{B}$ and can be regarded as an external force, and as such,

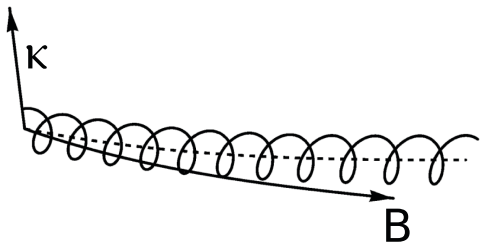

Figure 4. When the field line is curved (characterised by the curvature vector $\boldsymbol{\kappa}$), the particle undergoes a curvature drift. Dashed line represents the guiding centre trajectory.

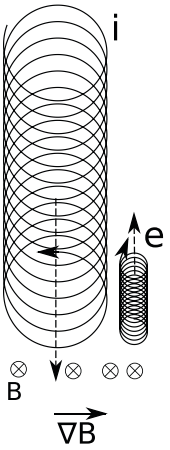

Figure 5. Grad-B drift of an ion, i, and an electron, e, in the presence of a straight $\boldsymbol{B}$ field with B increasing from left to right. Note that the two particle species drift in the opposite direction. Guiding centre orbits are represented by the dashed lines.

it gives rise to a drift velocity, as shown in figure 4. Recalling equation (2.14) we get

$$\boldsymbol{V}_{\boldsymbol{\kappa}} = \frac{v_{\parallel}^2}{\omega_{\mathrm{c}}} \hat{\boldsymbol{b}} \times \boldsymbol{\kappa}. \tag{2.20}$$

This velocity, known as the curvature drift velocity, depends on the sign of the particle charge so that, when the corresponding flow is summed over plasma particle species, it represents a transverse current, $\boldsymbol{J}_{\perp}$ carried by the guiding centres.

2.6. Transverse gradients of $\boldsymbol{B}$

If B varies spatially, the local value of the Larmor radius $r_{\mathrm{L}} = mv_{\perp}/(ZeB)$ varies between various phases of the gyration, being consistently smaller where the magnetic field is stronger, thereby leading to a drift in the direction of $\boldsymbol{B}\times\boldsymbol{\nabla}B$; see figure 5.

The drift can be most easily calculated after introducing the magnetic moment μ of a particle, which we anticipate to be constant along the particle orbit (we will elaborate on its constancy in section 3). The particle gyration is equivalent to a circulating electric current in a clockwise sense, for either sign of the particle charge. The magnetic moment associated with this current loop is given by

$$\mu = \text{current} \times \text{area of loop} = \frac{Ze\omega_{\mathrm{c}}}{2\pi}\pi r_{\mathrm{L}}^2 = \frac{mv_{\perp}^2}{2B}, \tag{2.21}$$

and the direction of the associated magnetic field is counter to that of the external field, thus the magnetic moment vector is $\boldsymbol{\mu} = -\mu\hat{\boldsymbol{b}}$. That is, a charge-neutral assembly of many charged particles is diamagnetic. The force acting on a magnetic dipole is $\boldsymbol{F} = \boldsymbol{\nabla}(\boldsymbol{\mu}\cdot\boldsymbol{B}) = -\boldsymbol{\nabla}(\mu B)$. As μ is constant along the particle orbit, the particle experiences a force $\boldsymbol{F} = -\mu\boldsymbol{\nabla}B$. Regarding the transverse component of this force, as in the previous section, we obtain the cross field drift with a velocity from equation (2.14)

$$\boldsymbol{V}_{\boldsymbol{\nabla}B} = \mu\frac{\boldsymbol{B}\times\boldsymbol{\nabla}B}{ZeB^2} = \frac{v_{\perp}^2}{2\omega_{\mathrm{c}}}\hat{\boldsymbol{b}}\times\left(\frac{\boldsymbol{\nabla}_{\perp}B}{B}\right). \tag{2.22}$$

We observe that μB plays the role of a potential which, as we will see in section 3, is important for parallel dynamics as well.

Finally, we note that in magnetically confined plasmas with low normalized pressure, $\beta = 2\mu_0 p/B^2 \ll 1$, the curvature can be approximated as $\boldsymbol{\kappa} \approx (\boldsymbol{\nabla}_\perp B)/B$. Thus the curvature drift takes a qualitatively similar form to the grad-B drift:

$$\boldsymbol{V}_{\boldsymbol{\kappa}} \approx \frac{v_\parallel^2}{\omega_c} \hat{\boldsymbol{b}} \times \left(\frac{\boldsymbol{\nabla}_\perp B}{B} \right). \tag{2.23}$$

3. Adiabatic invariants

Hamiltonian systems often exhibit periodic motion. When such a system is perturbed very slowly compared to the time scale of the oscillation, a quantity can be identified that remains practically unchanged by the perturbations. This quantity is called *action* and its approximate constancy is referred to as adiabatic invariance. We will see that when a gyrating particle experiences variations in the fields—due to their explicit time dependence or due to the motion of the particle—on a time scale much longer than the gyro-period, the magnetic moment is such an *adiabatic invariant*. If the particle orbits have other types of periodicity as well, it is possible to identify further adiabatic invariants. These will provide valuable information on the long time behaviour of the particle.

3.1. Magnetic moment in time-varying magnetic fields

A temporal variation of $\boldsymbol{B}$ is associated with a spatial variation of $\boldsymbol{E}$, by Faraday's law

$$\boldsymbol{\nabla} \times \boldsymbol{E} = -\frac{\partial \boldsymbol{B}}{\partial t}. \tag{3.1}$$

Here, for simplicity, we assume that $E_\parallel = 0$ and that $\boldsymbol{E}_\perp = 0$ at the guiding centre position, so that there is no $\boldsymbol{V}_E$ drift. However, we should note that, with our present definition of the guiding centre position as a distance r_L apart from the instantaneous particle position, the guiding centre must also experience a gyro-frequency 'wobble' since $r_L(t)$ does itself vary in a time dependent field. This 'wobble' in the position of the guiding centre is small compared to the Larmor radius itself, and could be removed by employing more sophisticated definitions of the guiding centre than we have done here.

Dotting equation (2.5) with $\boldsymbol{v}_\perp$ we find

$$\frac{\mathrm{d}}{\mathrm{d}t}\left(\frac{m v_\perp^2}{2Ze} \right) = \boldsymbol{E} \cdot \boldsymbol{v}_\perp. \tag{3.2}$$

Thus the change in perpendicular energy in one gyro-period is

$$\delta\left(\frac{m v_\perp^2}{2} \right) = Ze \oint \boldsymbol{E} \cdot \boldsymbol{v}_\perp \mathrm{d}t = Ze \oint \boldsymbol{E} \cdot \mathrm{d}\boldsymbol{l}, \tag{3.3}$$

where the loop integral is taken over one period of the gyro-orbit. Using Stokes' theorem, and Faraday's law equation (3.1), this becomes

$$\begin{aligned} \delta\left(\frac{m v_\perp^2}{2} \right) &= Ze \iint (\boldsymbol{\nabla} \times \boldsymbol{E}) \cdot \mathrm{d}\boldsymbol{S} = -Ze \iint \frac{\partial \boldsymbol{B}}{\partial t} \cdot \mathrm{d}\boldsymbol{S} \\ &= Ze \frac{\partial B}{\partial t} \pi r_L^2 = \frac{m v_\perp^2}{2} \frac{2\pi}{\omega_c} \frac{1}{B} \frac{\partial B}{\partial t}. \end{aligned} \tag{3.4}$$

Now the change in B over one gyro-period is just

$$\delta B = \frac{\partial B}{\partial t} \delta t = \frac{\partial B}{\partial t} \frac{2\pi}{\omega_c}, \tag{3.5}$$

so that we finally obtain

$$\delta\left(\frac{m v_\perp^2}{2} \right) = \frac{m v_\perp^2}{2} \frac{\delta B}{B}, \tag{3.6}$$

showing that

$$\delta\mu = 0, \qquad \text{or} \qquad \mu \equiv \frac{mv_\perp^2}{2B} = \text{constant}, \tag{3.7}$$

where μ is the magnetic moment introduced in equation (2.21). In other words, if the particle experiences an increase in the magnetic field strength, its perpendicular velocity increases, due to the accelerating electromotive force, so that the magnetic moment remains unchanged.

3.2. Magnetic moment in inhomogeneous magnetic fields

Recalling that we assume the magnetic field to be in the z direction at the gyro-centre (B_x and B_y vanish at $x = 0 = y$), and taking the z-component of equation (2.1) gives

$$\begin{aligned}\frac{m}{Ze}\dot{v}_z &= v_x B_y - v_y B_x = v_x y\frac{\partial B_y}{\partial y} - v_y x\frac{\partial B_x}{\partial x} \\ &= \frac{v_\perp^2}{\omega_c}\left[\cos^2(\omega_c t+\varphi)\frac{\partial B_y}{\partial y} + \sin^2(\omega_c t+\varphi)\frac{\partial B_x}{\partial x}\right],\end{aligned} \tag{3.8}$$

after using equations (2.10) and (2.11), and assuming that all other components of $\boldsymbol{\nabla B}$ are zero, except for $\partial_z B_z$, which must be finite, since $\boldsymbol{\nabla\cdot B} = 0$. Now, averaging over a gyro-period and using $\boldsymbol{\nabla\cdot B} = 0$ we have

$$\frac{m}{Ze}\dot{v}_z = -\frac{mv_\perp^2}{2ZeB}\frac{\partial B_z}{\partial z}. \tag{3.9}$$

Now, in the absence of an electric field the kinetic energy of the particle, $K = mv^2/2 = m(v_z^2 + v_\perp^2)/2$ is conserved, so we use

$$\frac{\mathrm{d}}{\mathrm{d}t}\left(mv_\perp^2\right) = -\frac{\mathrm{d}}{\mathrm{d}t}\left(mv_z^2\right) = -2mv_z\dot{v}_z, \tag{3.10}$$

in combination with equation (3.9), and using $B \simeq B_z$ at the guiding centre, so that $\mathrm{d}B/\mathrm{d}t = v_z\partial B_z/\partial z$, to deduce that

$$\frac{\mathrm{d}}{\mathrm{d}t}\left(\frac{mv_\perp^2}{2B}\right) \equiv \frac{\mathrm{d}\mu}{\mathrm{d}t} = 0. \tag{3.11}$$

Thus, as in the time dependent case discussed earlier, the magnetic moment is approximately constant for particles in inhomogeneous magnetic fields.

As a consequence of the constancy of the magnetic moment, μ, and the kinetic energy, $K = \frac{1}{2}mv^2$, we can express the parallel velocity of a particle as

$$v_\parallel = \sigma\sqrt{\frac{2}{m}(K - \mu B)} \tag{3.12}$$

where $\sigma = \pm 1$ represents the sign of $v_\parallel$. Since K and μ are both constant on the particle trajectory, equation (3.12) implies that $v_\parallel$ varies along the orbit in a spatially inhomogeneous magnetic field. Consequently, as a charged particle moves along a magnetic field into regions of stronger field B, its longitudinal velocity must diminish, and reflection will occur at a point where $B(\boldsymbol{x}) = K/\mu$. This is the magnetic mirror effect. It was exploited in early linear fusion research devices, called mirror machines, for parallel particle confinement. It also plays a significant role in tokamak plasmas, and is of great importance in understanding particle dynamics in Earth's magnetosphere.

It is important to note however, that the two constants K and μ, which result in the prediction of mirror reflection in inhomogeneous magnetic fields, are of a very different character. Provided there are no electric fields, and that we can neglect the effect of radiation reaction (to be discussed in section 4), the energy K is an exact constant of the motion. On the other hand, the magnetic moment, μ, has only been shown to be 'approximately constant'. In fact, μ is an example of an adiabatic invariant, the first of three that will appear in this section. Its approximate constancy is a much more subtle property than the constancy of K, as we will explain in the following.

It has been shown in Berkowitz *et al* (1959), Gardiner (1959), Kruskal (1962) that μ is the leading term of an asymptotic series in the small parameter, $\epsilon = r_L/L$, and that this series

$$\mu_*(\epsilon) = \mu + \epsilon\mu_1 + \epsilon^2\mu_2 + \ldots \tag{3.13}$$

is constant to all orders in ϵ. This does not, however, mean that μ_* is an exact constant, but that

$$\lim_{\epsilon\to 0}\left[\frac{\mu_* - \text{const.}}{\epsilon^N}\right] = 0, \quad \text{for any } N, \tag{3.14}$$

i.e. the deviation from constancy, $\Delta\mu = (\mu_* - \text{const.})$, goes to zero faster than any power of ϵ as $\epsilon \to 0$. Nevertheless, when ϵ is not asymptotically small, μ_* can experience jumps from time to time, which are exponentially small in ϵ, while it remains nearly constant between these jumps, as shown by Howard (1968), Hastie *et al* (1969).

In the following sections we will outline a systematic method for calculating the higher order corrections, $\mu_1(\boldsymbol{x},\boldsymbol{v}), \mu_2(\boldsymbol{x},\boldsymbol{v}), \ldots$, in the invariant series. In doing so, we shall discover the existence of the second and third adiabatic invariants referred to above.

3.3. Theory of adiabatic invariants

Here we discuss a systematic method to find higher order corrections to adiabatic invariants. The method we shall use is important since it is also used in the linear stability analysis of micro-instabilities. A mathematically rigorous and systematic development of the guiding centre equations has been described in more detail in Bogolyubov *et al* (1955, 1961), and alternative derivations regarding adiabatic invariants can be found in Northrop (1963), Sivukhin (1965).

To obtain the most general invariant, I, as a series expansion, in static but inhomogeneous fields, we solve

$$\frac{\mathrm{d}I}{\mathrm{d}t} = 0, \tag{3.15}$$

that is, the total variation of I along the particle orbit is zero, or equivalently

$$\boldsymbol{v}\cdot\boldsymbol{\nabla}I + \frac{Ze}{m}(\boldsymbol{v}\times\boldsymbol{B})\cdot\frac{\partial I}{\partial \boldsymbol{v}} = 0, \tag{3.16}$$

by expansion in powers of ϵ,

$$I = I_0 + \epsilon I_1 + \epsilon^2 I_2 + \ldots \tag{3.17}$$

Note that the first term in equation (3.16) is $\sim\epsilon$ smaller than the second (assuming that I is not sharply varying in phase space, i.e. $|\boldsymbol{\nabla}I| \sim I/L$ and $|\partial_{\boldsymbol{v}} I| \sim I/v$). It is worth mentioning that equation (3.16) is the Vlasov operator $\partial_t + \boldsymbol{v}\cdot\boldsymbol{\nabla} + (Ze/m)(\boldsymbol{v}\times\boldsymbol{B})\cdot\partial_{\boldsymbol{v}}$ acting on I (that has no explicit time dependence). When it operates on the distribution function $f(\boldsymbol{x},\boldsymbol{v},t)$, it gives the collisionless kinetic equation, or Vlasov equation, for the distribution function of charged particles in the given fields. Accordingly, solutions of equation (3.16) will have obvious applications in the kinetic theory of equilibria, and in linear stability analysis.

We consider the simplest case with no electric fields so that the energy $K = mv^2/2$ is an exact constant, and it is convenient to transform to the velocity space variables $\{\mu, K, \varphi\}$, where φ is the phase angle of the gyro-motion. Thus

$$\boldsymbol{v} = v_\parallel \hat{\boldsymbol{b}} + v_\perp\left(\hat{\boldsymbol{e}}_x\cos\varphi + \hat{\boldsymbol{e}}_y\sin\varphi\right), \tag{3.18}$$

where

$$v_\parallel = \sigma\sqrt{\frac{2}{m}(K-\mu B)}, \qquad v_\perp = \sqrt{\frac{2\mu B}{m}}, \tag{3.19}$$

and $\hat{\boldsymbol{e}}_x$ and $\hat{\boldsymbol{e}}_y$ are unit vectors normal to $\hat{\boldsymbol{b}}$ and to each other.

In real space it will be convenient to use a coordinate system associated with the magnetic field structure. Thus we introduce $\{\alpha, \beta, l\}$ where

$$\boldsymbol{B} = \boldsymbol{\nabla}\alpha\times\boldsymbol{\nabla}\beta \tag{3.20}$$

and l measures arc length along $\boldsymbol{B}$. Using these coordinates equation (3.16) takes the form

$$\omega_c\frac{\partial I}{\partial\varphi} = \mathscr{D}I, \tag{3.21}$$

where $\mathscr{D}$ is a complicated differential operator (details can be found in Hastie *et al* (1969)) of the form

$$\boldsymbol{v}\cdot\boldsymbol{\nabla} + D(\varphi,\mu,K)\frac{\partial}{\partial\mu} + A(\varphi,\mu,K)\frac{\partial}{\partial\varphi}, \tag{3.22}$$

with $\boldsymbol{v}$ given by equations (3.18) and (3.19), and the gradient operator is to be taken holding φ, μ and K constant. The function D has zero gyro-phase average, $\langle D\rangle = 0$, but $\langle A\rangle \equiv \bar{A} \neq 0$.

We solve equation (3.21) perturbatively in the smallness of ϵ, thus I is expanded as in equation (3.17). Realizing that the right hand side of equation (3.21) is ϵ smaller than the left hand side, we obtain to lowest order

$$\omega_c\frac{\partial I_0}{\partial\varphi} = 0, \tag{3.23}$$

implying that I_0 is gyrophase independent; most generally the solution is of the form $I_0 = I_0(\mu,K,\alpha,\beta,l)$. In effect this equation states that any function of the variables μ, K, α, β, and l remains constant on the gyration time scale, ω_c^{-1}. To next order one obtains

$$\omega_c\frac{\partial I_1}{\partial\varphi} = \mathscr{D}I_0. \tag{3.24}$$

Now since I_1 must be a periodic function of φ, there is an integrability condition associated with equation (3.24). This is obtained by annihilating $\partial_\varphi I_1$ by integrating over a period of φ, yielding

$$\langle\mathscr{D}I_0\rangle = 0, \tag{3.25}$$

and hence,

$$v_\parallel\frac{\partial I_0}{\partial l} = 0. \tag{3.26}$$

To obtain this result, stating the constancy of I_0 along the field line, we act with the operator of equation (3.22) on I_0 and gyro-average, then recall that $\langle D\rangle = 0$ and $\partial_\varphi I_0 = 0$, and from equation (3.18) that $\langle\boldsymbol{v}\rangle = v_\parallel\hat{\boldsymbol{b}}$. Thus, although equation (3.24) appears to be an equation for I_1, it also contains further information on the functional dependence of I_0, which must now be of the form

$$I_0 = I_0(\mu,K,\alpha,\beta). \tag{3.27}$$

Solving for I_1 by integrating equation (3.24) in φ gives

$$I_1 = \frac{1}{\omega_c}\int^\varphi \mathscr{D}I_0\mathrm{d}\varphi' + \bar{I}_1(\mu,K,\alpha,\beta,l), \tag{3.28}$$

where the integration constant $\bar{I}_1$—the gyrophase independent piece in I_1—is, as yet, unknown.

Thus, if we had chosen I_0 to be the magnetic moment, μ, equation (3.28) gives the oscillatory (i.e. φ dependent) part of the first correction, $\tilde{\mu}_1$, explicitly, although the complete first correction, $\mu_1 = \tilde{\mu}_1 + \bar{\mu}_1$, is not yet fully determined.

Proceeding to next order in the ϵ expansion, we obtain the equation

$$\omega_c\frac{\partial I_2}{\partial\varphi} = \mathscr{D}I_1. \tag{3.29}$$

Clearly in this order we begin to construct I_2, the second order correction to I_0 in the series expansion of the invariant, I, but again, there is an integrability condition obtained by annihilating the left hand side and employing equation (3.28)

$$\langle\mathscr{D}I_1\rangle = \langle\mathscr{D}\bar{I}_1\rangle + \left\langle\mathscr{D}\frac{1}{\omega_c}\int^\varphi \mathscr{D}I_0\mathrm{d}\varphi'\right\rangle = 0, \tag{3.30}$$

where explicit evaluation leads to the following result

$$v_\parallel\frac{\partial\bar{I}_1}{\partial l} + \boldsymbol{v}_\mathrm{d}\cdot\boldsymbol{\nabla}I_0 = 0, \tag{3.31}$$

with the magnetic drift velocity $\boldsymbol{v}_\mathrm{d}$ being precisely the sum of the two transverse guiding-centre drift velocities, the curvature drift and the grad-B drift velocities of equations (7.5) and (7.6), i.e.

$$\boldsymbol{v}_\mathrm{d} \equiv \boldsymbol{V}_{\boldsymbol{\kappa}} + \boldsymbol{V}_{\boldsymbol{\nabla} B}. \tag{3.32}$$

That is, the variation of $\bar{I}_1$ along the field line is caused by the variation of I_0 as the particle drifts across the magnetic field. Equation (3.31) now determines the hitherto undetermined part of I_1. However, if the longitudinal motion of the particle is periodic, equation (3.31) also has an integrability condition since the $\bar{I}_1$ term can be annihilated by integrating $\oint \mathrm{d}l/v_\parallel$ round the closed orbit. Periodicity in l may arise in two ways; either because the magnetic lines are themselves closed loops, or because mirror reflection returns the particle to its initial position. In either case the constraint condition takes the form:

$$\oint \frac{\mathrm{d}l}{v_\parallel} \boldsymbol{v}_\mathrm{d} \cdot \boldsymbol{\nabla} I_0 = 0, \tag{3.33}$$

where I_0 has already been constrained by equations (3.23) and (3.26) to have functional dependence of the form $I_0(\mu, K, \alpha, \beta)$. To understand the meaning of the new constraint, equation (3.33), we consider the particular case of a vacuum magnetic field. For this case $\boldsymbol{B}$ may be written as the gradient of a magnetic scalar potential

$$\boldsymbol{B} = \boldsymbol{\nabla} \chi, \tag{3.34}$$

where the surfaces of constant χ are orthogonal to those of the α and β coordinates, ($\boldsymbol{\nabla}\alpha \cdot \boldsymbol{\nabla}\chi = 0 = \boldsymbol{\nabla}\beta \cdot \boldsymbol{\nabla}\chi$). When $\boldsymbol{B}$ is the vacuum field, the low normalized pressure result for the curvature drift can be used, and the total magnetic drift reduced to the form

$$\boldsymbol{v}_\mathrm{d} = \boldsymbol{V}_{\boldsymbol{\nabla} B} + \boldsymbol{V}_{\boldsymbol{\kappa}} = \left(v_\parallel^2 + \frac{v_\perp^2}{2} \right) \frac{m}{ZeB^3} \boldsymbol{B} \times \boldsymbol{\nabla} B = -\frac{m v_\parallel}{ZeB} \boldsymbol{B} \times \boldsymbol{\nabla} \left(\frac{v_\parallel}{B} \right), \tag{3.35}$$

where we recalled the components of the drift, equations (2.22) and (2.23), and calculated $2v_\parallel \boldsymbol{\nabla} v_\parallel = \boldsymbol{\nabla} v_\parallel^2$ keeping K and μ constant when $\boldsymbol{\nabla}$ acts on $v_\parallel(\mu, K, B)$, as given by equation (3.12). Inserting the form of $\boldsymbol{v}_\mathrm{d}$ into equation (3.33) yields

$$\oint \frac{\mathrm{d}\chi}{B^2} \boldsymbol{B} \times \boldsymbol{\nabla} \left(\frac{v_\parallel}{B} \right) \cdot \boldsymbol{\nabla} I_0 = 0. \tag{3.36}$$

Finally, expressing the gradient operators as

$$\boldsymbol{\nabla} = \boldsymbol{\nabla}\alpha \frac{\partial}{\partial \alpha} + \boldsymbol{\nabla}\beta \frac{\partial}{\partial \beta} + \boldsymbol{\nabla}\chi \frac{\partial}{\partial \chi}, \tag{3.37}$$

using $\boldsymbol{B} = \boldsymbol{\nabla}\alpha \times \boldsymbol{\nabla}\beta$, and the orthogonality relations following equation (3.34), this becomes

$$\frac{\partial I_0}{\partial \alpha} \frac{\partial J}{\partial \beta} - \frac{\partial I_0}{\partial \beta} \frac{\partial J}{\partial \alpha} = 0, \tag{3.38}$$

where

$$J \equiv \oint \frac{v_\parallel}{B} \mathrm{d}\chi \equiv \oint v_\parallel \mathrm{d}l. \tag{3.39}$$

To find this result we used $B^2 = |\boldsymbol{\nabla}\alpha|^2 |\boldsymbol{\nabla}\beta|^2 - (\boldsymbol{\nabla}\alpha \cdot \boldsymbol{\nabla}\beta)^2$, and made use of the fact that the α and β derivatives commute with the χ integral.

The result equation (3.38), stemming from the constraint equation (3.33), therefore requires that I_0 be of the form

$$I_0 = I_0(\mu, K, J), \tag{3.40}$$

where I_0 is the leading term of the most general form of invariant (in particular, J itself is a possible such invariant). Proceeding to higher orders in the expansion it transpires that no new constraints on I_0 are generated. Now, choosing I_0 to be μ or J and evaluating the higher order terms, I_1, I_2, etc, we may construct the asymptotic series for these adiabatic invariants. The corrections μ_1, μ_2 and J_1, found in the

literature, have all been constructed by this method. In addition, higher order corrections to the guiding centre velocity $\boldsymbol{v}_c$ can be obtained from equations analogous to equation (3.31)

$$\sum_{j=0}^{l} \boldsymbol{v}_j \cdot \boldsymbol{\nabla} I_{l-j} = 0, \tag{3.41}$$

where the low order contributions $\boldsymbol{v}_0 = v_\parallel \hat{\boldsymbol{b}}$ and $\boldsymbol{v}_1 = \boldsymbol{v}_d \equiv \boldsymbol{V}_{\boldsymbol{\kappa}} + \boldsymbol{V}_{\boldsymbol{\nabla} B}$ have already been encountered. Again, for μ or J to be adiabatic invariants in the presence of given perturbations, the particle should experience these perturbations as being weak along its orbit over the time scales of the cyclotron or the bounce motion, respectively.

The importance of the longitudinal invariant, J, is that the particles for which it exists (such as the trapped particles in tokamak equilibria) are constrained to drift on surfaces described by

$$J(\mu, K, \alpha, \beta) = \text{constant}, \tag{3.42}$$

so that much is learned about the particle trajectory over very long times without the need to integrate the equations of motion, either of the gyrating particle, or of its guiding-centre.

Another important application is the optimization of particle confinement in stellarators. In non-axisymmetric configurations the possibility for trapped particles to drift out from the confinement regions on collisionless orbits is a serious issue, especially since energetic particles, such as fusion produced alphas are more prone to this process. The optimization approach called quasi-omnigeneity (Cary *et al* 1997) aligns the contours of J with flux surfaces, thus trapped particles will remain close to a given flux surface on average over a bounce period. Such optimization was used in the design of W-7X, the largest stellarator in operation.

If the drift surfaces described by equation (3.42) are closed, the slow drift motion is also periodic, and yet another invariant exists. For the stationary fields we have been considering, this additional invariant is just the particle energy, K, but if there is slow time dependence of the fields so that energy is not a conserved quantity, it is the flux invariant Φ (the magnetic flux contained within the drift surface), which is an adiabatic invariant of the motion (see Hastie *et al* (1967) for details).

3.4. Particle motion in tokamaks

As an elementary example of the application of the foregoing orbit theory, we investigate the nature of electron and ion orbits in a tokamak. The magnetic field of a tokamak is made up of two, axisymmetric, components: a strong toroidal field, generated by external coils, and a somewhat weaker poloidal field generated by currents flowing in the plasma as well as the poloidal field coils. The geometry and an appropriate coordinate system are shown in figure 6. We will consider a tokamak with circular magnetic surfaces which, although simplistic, is sufficient for our illustrative purposes, while it remains analytically tractable. The cylindrical coordinates, $\{R, \phi, Z\}$ are centred on the axis of symmetry, while the local coordinates r and θ are commonly used to describe functional behaviour in a $\phi = \text{const.}$ poloidal cross section. In particular, particle and guiding centre trajectories are often shown as projections on such a constant ϕ surface (as ϕ is an ignorable coordinate with regard to particle dynamics due to the axisymmetry of the system). The point at which $r \to 0$ is known as the magnetic axis of the device. In terms of the coordinates $\{r, \theta, \phi\}$, the magnetic field has the approximate form

$$\boldsymbol{B} = \{0, B_\theta(r), B_0\} \left(1 - \frac{r}{R_0}\cos\theta\right), \tag{3.43}$$

where R_0 is the distance from the axis of symmetry to the magnetic axis, a distance which we will assume is much greater than r (this is often referred to as the 'large aspect ratio' approximation). The magnetic field lines lie on the nested surfaces of constant r, and spiral slowly around these surfaces, whilst also spiraling around the axis of symmetry of the torus. The rate of this spiraling is obtained from

$$\frac{r\mathrm{d}\theta}{B_\theta} = \frac{R\mathrm{d}\phi}{B_0} \tag{3.44}$$

yielding $\mathrm{d}\phi/\mathrm{d}\theta = rB_0/[R_0 B_\theta(r)] = q(r)$, where $q(r)$ is the winding number, but is universally referred to as the 'safety factor' because of its important role in the magnetohydrodynamic stability of tokamaks. This quantity is of order unity in a tokamak, and it is typically a monotonically increasing function of r, assuming values from a little below 1 at the magnetic axis to $3-5$ towards the edge. This means that

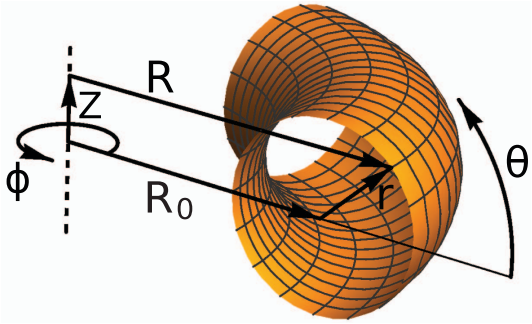

Figure 6. Toroidal and cylindrical coordinate systems for a circular cross-section tokamak. R: major radius, r: minor radius, θ: poloidal angle, ϕ: toroidal angle (note that it is sometimes defined clockwise to make $\{r, \theta, \phi\}$ right-handed), Z: elevation, R_0: major radius of the magnetic axis.

in a tokamak the toroidal component of the magnetic field is significantly stronger than the poloidal component, since $B_\theta = B_0(r/R_0)/q \ll B_0$.

In such a magnetic field, electrons and ions will, to leading order in r_L/L, follow magnetic field lines, gyrating around them with constant energy K and magnetic moment μ. Their guiding centre motion is described by equations (7.1)–(7.6). In terms of $\dot{r}$, $\dot{\theta}$, $\dot{\phi}$, we obtain

$$R\dot{\phi} = v_\parallel \frac{B_0}{B} - \frac{B_\theta}{B} v_\parallel \frac{\partial}{\partial r}\left(\frac{v_\parallel}{\omega_\mathrm{c}}\right), \tag{3.45}$$

$$r\dot{\theta} = v_\parallel \frac{B_\theta}{B} + \frac{B_0}{B} v_\parallel \frac{\partial}{\partial r}\left(\frac{v_\parallel}{\omega_\mathrm{c}}\right), \tag{3.46}$$

$$\dot{r} = \frac{B_0}{B}\frac{v_\parallel}{r}\frac{\partial}{\partial \theta}\left(\frac{v_\parallel}{\omega_c}\right). \tag{3.47}$$

Here we used the approximate form of $\boldsymbol{v}_\mathrm{d}$ given in equation (3.35). Thus the particle motion consists of a parallel streaming along the field line, plus a drift that is $\mathcal{O}(r_\mathrm{L}/L)$ smaller, and is mostly vertical for $B_\theta/B_0 \ll 1$. Note though that the drift also has a toroidal component, since the field lines are not purely toroidal.

As particles move poloidally towards regions with higher B their perpendicular energy $mv_\perp^2/2 = \mu B$ increases. By definition, $K \geqslant \mu B$ should be satisfied for all particles. From equation (3.43) the relative variation of B over the magnetic surface is $(B_\mathrm{i} - B_\mathrm{o})/\bar{B} \approx 2\varepsilon$, where $B_\mathrm{i} = B(r, \theta = \pi)$, $B_\mathrm{o} = B(r, \theta = 0)$, $\bar{B} \approx B(r, \theta = \pi/2)$ is the average B on the surface, and $\varepsilon = r/R_0$ (not to be confused with $\epsilon = r_\mathrm{L}/L$) is assumed to be small. The particles for which $1 - (\mu B_\mathrm{o}/K) < 2\varepsilon$ on the outboard side will reach $\mu B = K$ at some θ, where their $v_\parallel$ vanishes. Such particles are referred to as trapped particles and on any given magnetic surface ($r = $ const.) they constitute a fraction $\sim \sqrt{2\varepsilon}$ of all the particles in an isotropic distribution. They have a significant effect on many phenomena observed in tokamak plasmas. The remaining particles, referred to as passing particles, circulate in both θ and ϕ around the magnetic axis and the symmetry axis, without ever changing the sign of $v_\parallel$. However, although trapped particles reverse their parallel velocity, and consequently their motion in the toroidal direction, they nevertheless access all values of ϕ due to their precessional drift, which is described by the toroidal drift term in equation (3.45). This precession is illustrated in figure 7 that shows how the upper bounce point of a trapped particle moves around toroidally in consecutive periods of the trapped orbit.

For more general magnetic geometries it is useful to define a quantity ψ that is the flux of the poloidal magnetic field between the magnetic axis and any line on a given magnetic surface that closes on itself in a single toroidal turn (and makes no poloidal turns). The poloidal flux ψ is constant on a magnetic surface by construction, and can be used as a generalization of the minor radius coordinate r, since it monotonically increases from the magnetic axis outward (with $|\nabla\psi| = R|B_\theta|$).

As for any continuous symmetry of a physical system, the toroidal symmetry of the tokamak implies the existence of a quantity that is conserved along the particle orbits. This is called the canonical angular momentum

$$\psi_* = \psi - mRv_\phi/(Ze) \approx \psi - mRv_\parallel/(Ze), \tag{3.48}$$

where we have approximated ψ_* by its average over a gyro-period, and assumed $\boldsymbol{B}$ to be dominated by its toroidal component. As a consequence of the constancy of ψ_*, changes in $v_\parallel$ due to the mirror force

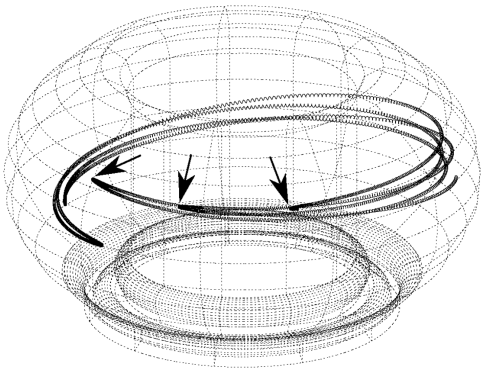

Figure 7. Toroidal precession of trapped particles. The upper bounce points of three consecutive periods of a trapped ion orbit are marked by arrows.

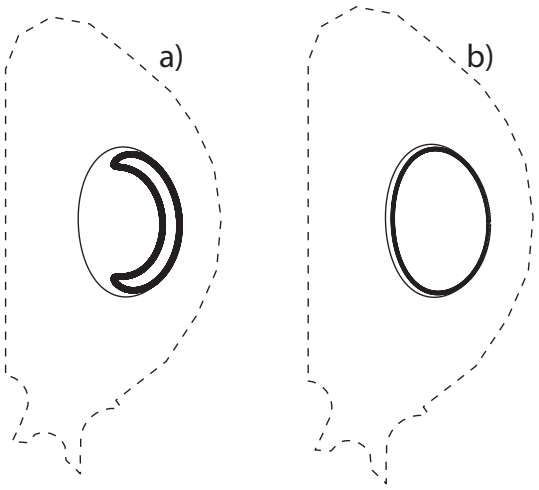

Figure 8. Poloidal projection of a trapped (a) and a passing (b) particle orbit in a tokamak. The figures correspond to 3.5 MeV fusion alpha particles in the ITER tokamak (for typical thermal particles the cross-field drifts would be invisible on this scale). Solid line: particle orbit, thin line: magnetic surface, dashed line: vacuum chamber.

lead to changes in ψ, that is, the particle will drift radially—consistently with the circular geometry result equation (3.47). Since the changes in $v_{\|}$ are bounded, and $mRv_{\|}/Ze\psi \sim |B/B_\theta|(r_\mathrm{L}/r) \equiv r_{\mathrm{L}\theta}/r$, the particle will stay in the vicinity of some magnetic surface. We have introduced the poloidal Larmor radius $r_{\mathrm{L}\theta} = |B/B_\theta| r_\mathrm{L}$ which is larger than r_L, but still much smaller than the minor radius of the device.

For circulating particles the poloidal variation of $v_{\|}$ is $\Delta v_{\|} \sim \varepsilon v$, so the excursion of the particle from the flux surface $\Delta r \sim \Delta\psi/|\nabla\psi| \approx \Delta\psi/(R_0 B_\theta) \sim m\Delta v_{\|}/(ZeB_\theta) \sim \varepsilon\, r_{\mathrm{L}\theta}$. Trapped particles have $v_{\|} \sim \sqrt{\epsilon} v$, and since their $v_{\|}$ changes sign along their orbit $\Delta v_{\|} \sim v_{\|} \sim \sqrt{\epsilon} v$. This leads to larger drift departures compared to the circulating particles $\Delta r \sim \sqrt{\epsilon} r_{\mathrm{L}\theta}$. Even though the particles drift in the same direction all the time (nearly vertically), their orbits are such that they move away from a magnetic surface half of the time, and then move back towards it. As a result, the poloidal projection of their orbits is a closed curve, as seen in figure 8.

4. Radiation reaction effects

Throughout the foregoing discussion, we have ignored all radiation processes. As a consequence the particle energy was found to be an exact constant of particle motion for electrons and ions moving in static fields if $\boldsymbol{E}\cdot\boldsymbol{B} = 0$ (or, more generally for zero longitudinal force), and the magnetic moment was found to be an approximate constant of motion. However, since an accelerating charge radiates energy in

the form of electromagnetic waves, it loses energy at a rate (see Bekefi (1966))

$$\frac{\mathrm{d}K}{\mathrm{d}t} = \frac{Z^2 e^2}{6\pi\epsilon_0 c^3} a^2 \tag{4.1}$$

where a is the acceleration. As we have seen, all charged particles are being continuously accelerated by the magnetic field with $\boldsymbol{a} = (Ze/m)\boldsymbol{v}\times\boldsymbol{B}$. The resulting radiation is termed cyclotron radiation, or, for relativistic particles synchrotron radiation, and it causes a gradual energy loss. Thus, integrating equation (4.1) for a non-relativistic particle we obtain the result

$$K_\perp(t) = K_{\perp 0}\exp(-t/\tau_R), \tag{4.2}$$

where $K_\perp = mv_\perp^2/2$ is the energy of gyration of the particle, and the characteristic time τ_R for radiative energy loss is

$$\tau_\mathrm{R} = \frac{3\pi\epsilon_0 mc^3}{e^2\omega_c^2}. \tag{4.3}$$

Since τ_R scales as m^3, this energy loss process can only be of significance for electrons. For conditions typical of most fusion devices τ_R lies in the range $\sim$1-10 s and is therefore considerably longer than other timescales characteristic of electron orbits. In addition, these expressions overestimate the rate of energy loss of an electron, since local absorption of the radiation from neighbouring electrons also takes place. This inverse process is exploited in radio-frequency heating schemes in fusion devices, where intense radio frequency waves at the cyclotron frequency of ions or electrons, or at low harmonics of this frequency, are launched into the plasma and are resonantly absorbed by the gyrating particles.

Even though the thermal electron population in a tokamak is non-relativistic, under certain unwanted circumstances a relativistic population of electrons, so called runaway-electrons, may be generated. The possible energization of these particles relies on that the effect of Coulomb 'collisional' interactions on particle trajectories becomes weaker with increasing speed. This counter-intuitive feature is a result of Debye screening (to be discussed in section 5), as faster particles have less time to spend in each others vicinity, where they can interact. Therefore the force corresponding to an induced toroidal electric field may not be balanced by collisional friction with thermal particles, and a population of super-thermal electrons are freely accelerated. Thus for runaway electrons—which can reach energies of tens of MeV—radiation reaction can significantly affect their dynamics (Hirvijoki *et al* 2015). Namely, synchrotron radiation reaction limits the achievable highest energy of the runaways, above which their number drops exponentially. In certain cases it can lead to a pile-up of electrons at a certain energy leading to a non-monotonic energy dependence (Decker *et al* 2016).

5. Debye screening and quasineutrality

So far we have considered the dynamics of particles in isolation in the presence of given electric and magnetic fields. Due to the contribution of particles to the fields, and their response to fields generated by other particles, plasmas exhibit *collective behaviour*. This means that, unlike gases, where the motion of particles is essentially random, and particles only interact through instantaneous binary collisions, plasma particles collectively respond to self-consistent fields which can lead to large-scale, coherent dynamics. One important feature of plasmas is that in any macroscopic volume the plasma is extremely close to be charge neutral. We will now quantify 'macroscopic' in this context, by calculating the response of a plasma to the introduction of additional charge. This leads us to the phenomenon known as Debye screening and the concept of quasineutrality.

The Coulomb potential of a particle of charge Ze in vacuum is $\phi = Ze/(4\pi\epsilon_0 r)$. If this particle is introduced into a homogeneous plasma, it attracts electrons and repels ions in such a way that its electrostatic potential is attenuated at distances beyond a characteristic length, called the Debye length. To calculate this effect we solve for the potential, $\phi(r)$ generated by such a test charge, as a function of the distance from the charge r. For simplicity we assume the plasma to be in thermal equilibrium, with the distribution functions of electrons and ions being Maxwell–Boltzmann with the same temperature T

$$f_j(\boldsymbol{x},\boldsymbol{v}) = f_j(r,v) = n_j\left(\frac{m}{2\pi T}\right)^{3/2}\exp\left(-\frac{mv^2}{2k_\mathrm{B}T} - \frac{Z_j e\phi(r)}{k_\mathrm{B}T}\right), \tag{5.1}$$

where j is a species index, and we made the spherical symmetry of the problem explicit. The densities corresponding to equation (5.1) are $n_j(r) = n_{j0}\exp[-Z_j e\phi/(k_\mathrm{B}T)]$. The potential generated by the test charge, $\phi(r)$ is, as yet, unknown. Since the potential must satisfy Poisson's equation

$$\nabla^2\phi(r) = -\frac{\rho_\mathrm{e}(r)}{\epsilon_0} \qquad \text{for } r \neq 0, \tag{5.2}$$

where we excluded the location of the test charge, and introduced the total charge $\rho_\mathrm{e} = \sum_j Z_j e n_j$. For simplicity, let us consider a hydrogenic plasma, with one singly charged ion species ($Z_\mathrm{i} = 1$, $Z_\mathrm{e} = -1$). Furthermore, we assume the plasma to be neutral without the presence of the test charge ($n_{\mathrm{e}\,0} = n_{\mathrm{i}\,0} = n_0$). Then $\rho_\mathrm{e} = -2en_0\sinh[e\phi/(k_\mathrm{B}T)] \approx -2e^2n_0\phi/(k_\mathrm{B}T)$, where we expanded in the assumed smallness of $e\phi/(k_\mathrm{B}T)$. It follows that ϕ satisfies the equation

$$\frac{1}{r^2}\frac{\partial}{\partial r}r^2\frac{\partial\phi}{\partial r} = \frac{2e^2n_0}{\epsilon_0 k_\mathrm{B}T}\phi. \tag{5.3}$$

Taking the physically relevant solution of equation (5.3) that vanishes as $r \to \infty$, we obtain

$$\phi(r) = \frac{A}{r}\exp\left(-\frac{r}{\lambda_\mathrm{D}}\right), \tag{5.4}$$

where $\lambda_\mathrm{D} \equiv [\epsilon_0 k_\mathrm{B}T/(2n_0e^2)]^{1/2}$ is known as the Debye length. The constant A can be determined by matching the solution equation (5.4) to the 'bare' Coulomb potential of the test charge for values of r which are small compared to the average inter-particle distance, $\sim n_0^{-1/3}$, i.e. to $\phi = Ze/(4\pi\epsilon_0 r)$, which gives

$$\phi(r) = \frac{Ze}{4\pi\epsilon_0}\frac{1}{r}\exp\left(-\frac{r}{\lambda_\mathrm{D}}\right). \tag{5.5}$$

Here we assumed that $n_0^{-1/3} \ll \lambda_\mathrm{D}$, which means that there is a large number of particles 'inside the Debye sphere' of the test charge (i.e. within a range λ_D). This is the case for many high temperature plasmas of interest, such as for magnetic fusion plasmas. We note that while the expansion $e\phi/(k_\mathrm{B}T)$ is not strictly valid close to the test charge the distance where this approximation breaks down is smaller than the typical inter-particle distance, when $n_0^{-1/3} \ll \lambda_\mathrm{D}$ is satisfied.

Equation (5.4) then shows that, at distances greater than the Debye length, the potential of a test charge is exponentially attenuated below the value it would have in a vacuum. This cutoff of the potential has important implications for the binary Coulomb collisional events in a plasma, limiting them to interactions between particles which approach within a Debye length of each other. It also implies that each particle in a plasma is simultaneously undergoing many collisional encounters with all the particles within its Debye sphere, a number of order $n_0\lambda_\mathrm{D}^3$. For most laboratory and space plasmas this is a very large number, and is often used as the defining characteristic of a 'plasma'. In typical tokamaks, for example λ_D is of similar magnitude to the electron Larmor radius $\sim 10^{-5}$ m, while the average inter-particle distance $\sim 10^{-7}$ m.

We see that a non-magnetized plasma does not support macroscopic (i.e. larger than Debye scale) charge accumulation; accordingly, it is called 'quasineutral'. If the particles are free to move they do so such that by rearranging their positions they cancel electrostatic fields. In strongly magnetized plasmas the particles are tied to magnetic field lines and cannot easily rearrange to cancel perpendicular electrostatic fields, nevertheless the plasma stays quasineutral. If a charge imbalance were to occur due to processes that can cause charge separation across the magnetic field, an electrostatic field would immediately set up to restore charge imbalance: we have learned that an increasing electric field causes a polarization drift, that is essentially a shift in the guiding centre position due to a $\boldsymbol{V_E}$ drift, and this drift generates an increasing polarization charge density. Analogously, not only the particle gyration, but drifting guiding centre orbits can also lead to polarization. Such polarization processes continue until the charge imbalance is removed, leading to a quasineutral plasma with particles drifting in a perpendicular electrostatic field.

6. Particle orbits affected by collisions and fluctuations

Collisions in plasmas are qualitatively different from those in neutral gases. In the latter, collisions are essentially instantaneous and lead to an abrupt change in the momentum of the atoms or molecules.

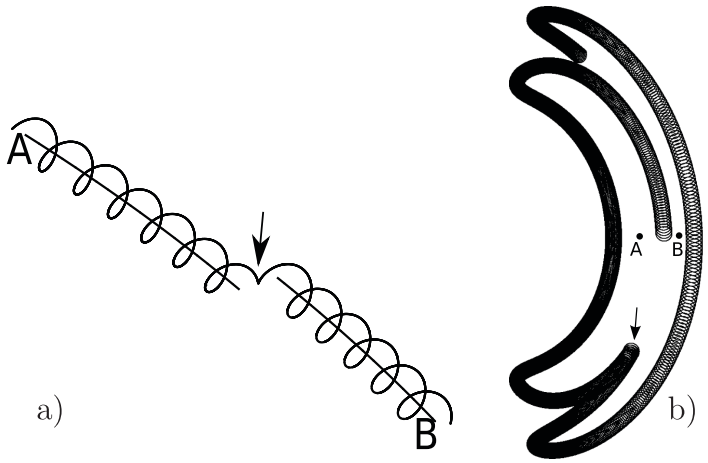

Figure 9. Collisional effects on particle orbits. Collisions occur at locations denoted by the arrows. (a) Particle jumps from guiding centre A to guiding centre B, which are separated by a distance $\sim r_\mathrm{L}$. (b) Poloidal projection of a particle jumping from one trapped orbit to another, with their average particle positions, denoted by A and B, separated by a distance $\sim \sqrt{\varepsilon}|B/B_\theta|r_\mathrm{L}$. Note that the collisions are depicted as instantaneous only to assist visualization.

In plasmas, each charged particle continuously and simultaneously interacts with a large number of other charged particles which are inside its Debye-sphere. The vast majority of these binary interactions cause only a very small change in the particle's momentum. As a result, the phase space trajectory of the particle is continuous and smooth. Therefore the collision time, which in gases would be the characteristic time between two consecutive collisions, needs to be re-defined: In plasmas, the collision time τ_c is the time needed for an order unity relative change in momentum as a cumulative effect due to the binary interactions. We can also define the collision frequency $\nu_\mathrm{c} = 1/\tau_\mathrm{c}$. Note that the collision frequency defined in this way is different between various particle species. For instance, to significantly change the momentum of an ion by collision with electrons takes much longer than to change the momentum of an electron as it collides with ions. In this way we may define collision frequencies such as $\nu_\mathrm{ie} \ll \nu_\mathrm{ii} \ll \nu_\mathrm{ei}$, where ν_{12} refers to the effect on species 1 due to collisions with species 2 (e and i denote electron and ion), and the separation between the listed frequencies is $\sim\sqrt{m_\mathrm{i}/m_\mathrm{e}}$.

The fields present on scales larger than the Debye length due to the collective behaviour of particles result in deterministic and reversible phase space dynamics. Collisions add a random component to the velocity trajectory of individual particles which, on a statistical level lead to diffusion in velocity space. This velocity diffusion is then also reflected in the configuration space dynamics. Even though collisions are not instantaneous in plasmas, to get a qualitative understanding of long term collisional effects, we will still visualize collisions as sudden events in the following.

The effect of a Coulomb collisional encounter resulting in a scatter of the gyro-angle of a charged particle is shown schematically in figure 9(a). The guiding centre experiences a jump that is comparable to r_L. The cumulative effect of such collisions on a test particle is that the guiding-centre undergoes a random walk, in which characteristic displacements of order r_L occur with frequency ν_c. Considering a large number of particles, such a random walk leads to a spatial diffusion of their guiding centres, and thus particle positions, with diffusion coefficient $D_\perp \sim \nu_\mathrm{c} r_\mathrm{L}^2$. This diffusion, which scales as B^{-2}, is known as classical diffusion, and it is present even in a straight magnetic field configuration. As the characteristic collision frequency for electrons is $\sqrt{m_\mathrm{i}/m_\mathrm{e}}$ larger than that for ions, while the electron Larmor radius is smaller by the same factor, it follows that $D_{\perp\mathrm{e}} \sim D_{\perp\mathrm{i}}\sqrt{m_\mathrm{e}/m_\mathrm{i}} \ll D_{\perp\mathrm{i}}$. Since the charge separation due to unequal diffusion rates would generate large electric fields, in practice charge separation induces electric fields to develop which restrain the ions and both charge species diffuse across the magnetic field at the slower rate characterized by electrons. This feature of the radial particle transport, that it does not lead to radial currents, is called *ambipolarity*. Other phenomena that cause cross-field transport, such as plasma turbulence, can also be ambipolar.

An interesting phenomenon occurs at the low collision frequencies of the high temperature plasmas in recent toroidal confinement devices. As we have seen in section 3.4 a change in $v_\parallel$ corresponds to a change in the radial location of the particle in a tokamak due to the conservation of the canonical angular momentum. In analogy to collisional changes in the gyro-phase leading to jumps in the particle orbit, collisional changes in $v_\parallel$ can lead to jumps between drift orbits, as illustrated in figure 9(b). For a collision to lead to a jump between two trapped drift orbits as shown in the figure, or to de-trap a

trapped particle, requires a change in $v_{\|}$ comparable to the trapped region in velocity space. This corresponds to an effective collision frequency $\nu_c' = \nu_c/\varepsilon$ that is higher than ν_c. In the corresponding random walk the step size is also larger, comparable to the trapped orbit width $r_L' = \sqrt{\varepsilon}|B/B_\theta|r_L$. Even though the trapped particles, for which the above considerations apply, constitute only an $f_t \sim \sqrt{\varepsilon}$ fraction of all the particles, the diffusion due to this process $D_\perp'$ is significantly larger than that from classical diffusion. We can estimate the diffusivity as $D_\perp' \sim f_t \nu_c' r_L'^2 \sim (q^2/\varepsilon^{3/2})\nu_c r_L^2 \gg D_\perp$, which is, similarly to classical diffusion, proportional to B^{-2} .

Particles in non-axisymmetric fields, especially the highly structured fields of stellarators, have the unfortunate opportunity to become trapped in localized regions of weak magnetic field. Their drift motion is no longer compensated on different segments of the orbit, which led to the closed poloidal projection shown in figure 6, but gives rise to a unidirectional motion and loss from the plasma. As collisions continually repopulate such *loss regions* of phase space, confinement can become unacceptably low. When the temperature is sufficiently low that collisions can frequently interrupt such drift motion, a random walk estimate of the transport finds that $D_\perp \propto 1/\nu_c$. This is unlike the symmetric regimes considered above, where collisions enabled cross-field transport. At higher temperatures, particle losses begin to generate a radial electric field—which introduces a new component to the drift motion, tangential to a flux surface. To operate successfully at the required high temperatures, stellarator configurations must therefore be optimized self-consistently, to keep trapped particles close to a given flux surface on an orbit average. A variety of regimes, with collisions once again enabling cross-field diffusion, can result (Helander 2014).

We have mostly considered processes in the presence of static fields, however in fusion plasmas there are turbulent fluctuations, which are responsible for most of the cross-field heat and particle flows. We will only briefly touch upon these in this chapter, in the context of particle orbits and collisions.

Turbulence in conventional tokamaks with small β is dominantly electrostatic, that is, while perturbations about the equilibrium magnetic field are tiny, there are low frequency fluctuations of the electrostatic potential. Particles drift in the corresponding fluctuating electric field, and undergo a random walk process, the magnitude of which depends on the size and decorrelation time of the fluctuations.

If particles could instantaneously respond to the electric field fluctuations they would rearrange themselves so as to cancel the fluctuations. This behaviour is called an *adiabatic response*. However due to the finite mass of the particles, the confining magnetic field, and collisions, particle dynamics deviates from adiabaticity, which is of key importance for the destabilization of the small scale instabilities—so called *microinstabilities*—that represent the drive for the fluctuations themselves. Circulating electrons are close to being adiabatic, since they can move very quickly along the field lines and rapidly respond to fluctuations. Trapped electrons, on the other hand, cannot move freely along the field line, therefore they behave non-adiabatically, and as such, they affect the micro-stability of the plasma. Even though their motion is limited in the poloidal direction, they have a toroidal precession. This makes it possible that they can get in resonance with drift waves propagating toroidally with a speed similar to their precession velocity. Such resonant electrons are responsible for the destabilization of the drift wave microinstabilities called trapped electron modes. Collisions which can move particles in and out from the trapped region of velocity space naturally affect the response of electrons, thus the micro-stability of the plasma.

7. Summary

In this chapter we have outlined the theory of charged particle motion in electromagnetic fields that are slowly varying on the time- and spatial scales of the gyration of the particle. We have seen that particle trajectories can be broken down into rapid gyration, together with equations describing the motion of the guiding centre, by expansion in the two parameters, r_L/L and ω/ω_c, with both assumed small. Any temporal and spatial variation of $\boldsymbol{E}$ and $\boldsymbol{B}$ give rise to slow, guiding-centre drift velocities— $\boldsymbol{E}\times\boldsymbol{B}$-drift, polarization drift, curvature drift and grad-B drift. With the exception of the $\boldsymbol{E}\times\boldsymbol{B}$-drift, these drifts induce charge separation and lead to the flow of transverse currents in the plasma.

When an accelerating parallel electric field is absent the guiding centre velocity is composed as follows

$$\dot{\boldsymbol{x}}_c = \boldsymbol{v}_c = v_{\|}\hat{\boldsymbol{b}} + \boldsymbol{V}_{\boldsymbol{E}} + \boldsymbol{V}_{\dot{\boldsymbol{E}}} + \boldsymbol{V}_{\boldsymbol{\kappa}} + \boldsymbol{V}_{\boldsymbol{\nabla}B}, \tag{7.1}$$

$$\hat{\boldsymbol{b}}\cdot\dot{\boldsymbol{x}}_c = v_{\|} = \sigma\sqrt{\frac{2}{m}(K-\mu B)}, \tag{7.2}$$

$$\boldsymbol{V}_{\boldsymbol{E}} = \frac{\boldsymbol{E}\times\boldsymbol{B}}{B^2}, \tag{7.3}$$

$$\boldsymbol{V}_{\dot{\boldsymbol{E}}} = \frac{1}{\omega_c}\frac{\dot{\boldsymbol{E}}}{B}, \tag{7.4}$$

$$\boldsymbol{V}_{\boldsymbol{\kappa}} = \frac{v_\parallel^2}{\omega_c}\hat{\boldsymbol{b}}\times\boldsymbol{\kappa}, \tag{7.5}$$

$$\boldsymbol{V}_{\nabla B} = \frac{v_\perp^2}{2\omega_c}\hat{\boldsymbol{b}}\times\left(\frac{\nabla B}{B}\right). \tag{7.6}$$

We have shown how, when the inhomogeneities in the fields are relatively weak, different characteristic times can be distinguished naturally, and approximate constants of motion—adiabatic invariants—can be constructed. The first adiabatic invariant—the magnetic moment, μ—is responsible for the phenomenon of mirror reflection in inhomogeneous fields. We have also briefly discussed the longitudinal invariant, J, and the flux invariant Φ, which appear if the particle motion exhibits periodicity on longer time scales than gyration (for example over the bounce motion of trapped particles). Using these adiabatic invariants allow us to make predictions about the nature of particle trajectories over long time scales without the need to actually integrate the equations of motion, as we have seen through examples in tokamak geometry.

We note that single-particle dynamics can also be formulated in a Lagrangian (or Hamiltonian) framework, which provides a particularly powerful and systematic approach, especially for deriving guiding-centre motion and adiabatic invariants. We refer the reader to standard texts such as Northrop (1963), Littlejohn (1983), Cary and Brizard (2009) for detailed treatments.

The total particle energy is a constant of motion only when particles do not interact or emit radiation. We briefly touched upon radiation reaction losses and their role in the dynamics of energetic electrons.

Towards the end of the chapter we went beyond the single particle picture and considered some effects of the collective behaviour in plasmas. We established that charges are Debye-screened in plasmas over a length that is larger than the average inter-particle distance, but much smaller than the characteristic scales of many phenomena of interest. Debye screening ensures that plasmas are quasineutral on macroscopic scales, and that the range of Coulomb collisions is limited to the Debye length.

Finally, we have considered how collisions affect particle orbits, and found that collisions lead to a diffusive cross particle transport. Magnetic geometry and orbit topologies play an important role in this context; even though there are typically fewer trapped particles than circulating ones, we have seen that they contribute much more to collisional transport. We also mentioned some aspects of turbulent fluctuations in relation to particle orbits and collisions.

Many complex phenomena in plasmas can be approached using fundamental ideas based on charged particle dynamics, and importantly, single particle dynamics lays the foundation for the kinetic theory of plasmas.

Data availability statement

No new data were created or analysed in this study.

Author contribution

R J Hastie
Conceptualization (equal), Methodology (equal), Writing – original draft (equal), Writing – review & editing (equal)

References

Abel I G, Plunk G G, Wang E, Barnes M, Cowley S C, Dorland W and Schekochihin A A 2013 *Rep. Prog. Phys.* **76** 116201
Bekefi G 1966 *Radiation Processes in Plasmas* (Wiley)
Berkowitz J and Gardiner C 1959 *Commun. Pure Appl. Math.* **12** 501
Bogolyubov N N and Mitropolskii Y A 1961 *Asymptotic Methods in the Theory of Nonlinear Oscillations* (Gordon and Breach)
Bogolyubov N N and Zubarev D N 1955 *Ukranian Math. J.* **7** 5–17
Cary J R and Brizard A J 2009 *Rev. Mod. Phys.* **81** 693
Cary J R and Shasharina S G 1997 *Phys. Rev. Lett.* **78** 674
Decker J, Hirvijoki E, Embreus O, Peysson Y, Stahl A, Pusztai I and Fülöp T 2016 *Plasma Phys. Control. Fusion* **58** 025016
Dubin D H E, Krommes J A, Oberman C and Lee W W 1983 *Phys. Fluids* **26** 3524

Gardiner C 1959 *Phys. Rev.* **115** 791
Hastie R J, Hobbs G D and Taylor J B 1969 *3rd Int Conf. on Plasma Physics and Contr. Fusion. Research* vol 6 (IAEA) p 389
Hastie R J, Taylor J B and Haas F A 1967 *Ann. Phys. NY* **41** 302
Helander P 2014 *Rep. Prog. Phys.* **77** 087001
Hirvijoki E, Pusztai I, Decker J, Embreus O, Stahl A and Fülöp T 2015 *J. Plasma Phys.* **81** 475810502
Howard J E 1968 *Phys. Fluids* **11** 1569
Kruskal M 1962 *J. Math. Phys.* **3** 806
Littlejohn R G 1983 *J. Plasma Phys.* **29** 111
Northrop T G 1963 *The Adiabatic Motion of Charged Particles* (Interscience)
Parra F I and Catto P J 2008 *Plasma Phys. Control. Fusion* **50** 065014
Sivukhin D V 1965 *Reviews of Plasma Physics* vol 1, ed M A Leontovich (Consultants Bureau) p 1